
Studies of concentration dependence of the fluorescent quantum yield from rhodamine 6G and Au–Pd core–shell nanorods, using a response surface methodology

Ekkachai Rammarat, Kitsakorn Locharoenrat, Witoon Yindeesuk and Pattareeya Damrongsak

Department of Physics, Faculty of Science, King Mongkut's Institute of Technology Ladkrabang, No. 1 Chalongkrung Road, Ladkrabang District, Bangkok 10520, Thailand, kitsakorn.lo@kmitl.ac.th

Received: 13.07.2017

Abstract. We have applied a response surface approach to study the fluorescence quantum yield (FQY) of rhodamine 6G (Rh6G) mixed with Au–Pd core–shell nanorods (Au–Pd NRs). The FQYs have been measured for the Rh6G concentrations varying from 3.53×10^{-7} to 1.70×10^{-6} mol/L and the concentrations of Au–Pd NRs from 7.06×10^{-6} to 1.36×10^{-4} mol/L. Our experimental results testify that the FQY depends notably on the proportions of Rh6G and Au–Pd NRs. A specific relationship between the FQY and the concentrations has also been confirmed by a response surface plot. It is found that the discrepancy between the experiment and the calculations is less than 2%.

Keywords: fluorescence, response surface methodology, nanorods

PACS: 33.50.Dq, 06.20.Dk, 78.67.Qa.

UDC: 535.37

1. Introduction

Interactions between metal nanoparticles and fluorophores have been extensively studied because they offer diverse applications in the fields of biosensors [1], cell imaging [2] and photovoltaics [3]. It has been reported that the emission intensity of fluorophores can be either enhanced or quenched when they are located near metal nanoparticles. This depends on the distance between the metal nanoparticles and the particles of fluorophores. Enhancement of fluorescent signals due to the presence of metal nanoparticles, which is referred to as a metal-enhanced fluorescence, is commonly attributed to excitation of surface plasmons on the metal surfaces [4]. Then the nanoparticles act as fluorescence amplifiers. On the other hand, another phenomenon known as a fluorescence resonance energy transfer can become dominant, whenever the fluorophores are in a close (less than 10 nm) proximity to the metal nanoparticles [5]. This effect leads to reduction, or even quenching, of the fluorescent signal.

A number of studies have been reported on the fluorescence enhancement and quenching caused by different metal nanoparticles. Suslov et al. [6] have shown that the fluorescence of rhodamine B is enhanced by monodispersed silver nanoparticles. Chen et al. [7] have found that silver nanoparticles can either enhance or quench the fluorescence of organic LEDs. Finally, Boonpi-phobanun et al. [8] have presented some results concerned with enhancement and quenching that occurs in the emission spectra of Au–Pd core–shell nanorods (Au–Pd NRs). Nevertheless, there are only few studies on the effect of metal nanoparticles upon one of the main fluorescence parameters, a fluorescent quantum yield (FQY). This parameter, which is given by the ratio of

number of the emitted photons to that of the absorbed photons, is very important for determining the efficiency of fluorophores. In particular, the influence of different concentrations of the metal nanoparticles on the FQY remains unknown. We intend to fill this gap in the present work. We are going to focus on the Au–Pd NRs mentioned above and rhodamine 6G (Rh6G) clusters in liquid solution, instead of solid matrices. We have restricted our analysis to Rh6G dye, since it offers a high FQY.

The FQY is usually derived using a relative method [9, 10]. The latter relies on measuring the signals obtained from an unknown sample and a reference sample, of which FQY is known under the same conditions. By comparing the fluorescence intensities detected from the sample with that from the reference, one can determine the FQY of the sample under test as

$$FQY = FQY_R \frac{I}{I_R} \frac{A_R}{A} \left(\frac{n}{n_R} \right)^2, \quad (1)$$

where I is the integrated fluorescence intensity, A the absorbance, n the refractive index of a solvent, and the subscript R refers to the reference fluorophore in all cases.

To examine possible relationships between the FQY and the proportions of Au–Pd NRs and Rh6G, a response surface methodology with a central composite design has been employed. The response surface methodology is a combination of statistical and mathematical techniques for improving and optimizing different processes [11]. The method has attracted a lot of attention because it is capable of determining both the individual and interactive effects of many factors of interest. Moreover, it requires a smaller number of experiments, if compared to conventional methods. For example, the response surface methodology has been used to study the effect of temperature on the thermoelectric properties [12] and to optimize production of biodiesel from the waste cooking oil [13]. In our study, we use the response surface methodology to create analytical model for the dependences of FQY on the Rh6G and Au–Pd NR concentrations. Then the accuracy of the model can easily be validated with the experimental data. Besides, such a model would be very useful when determining proper concentrations of mixture-sample solutions that enhance the FQY.

2. Experimental

An Rh6G dye powder was purchased from Sigma Aldrich, USA. No further purification was performed. An Rh6G stock solution (6×10^{-6} mol/L) was prepared by dissolving a desired quantity of the dye in deionised water. Au–Pd NRs were purchased from NonoSeedz Limited, Hong Kong. They had the diameters 40 ± 3 nm and the lengths 96 ± 6 nm.

As already mentioned, the influence of the concentration of Au–Pd NRs on the FQY of Rh6G was investigated using the response surface methodology based on the central composite design. A Design Expert Software 9.0.3 was employed for this aim. Since there were two input factors, Rh6G and Au–Pd NR concentrations ($k = 2$), the total number of samples needed for our experiments was equal to $2^k + 2k + n = 13$, with n being the number of replicated runs ($n = 5$) [14]. The dye stock solutions were prepared to obtain the test solutions with the concentrations ranging from 3.53×10^{-7} to 1.70×10^{-6} mol/L (see Table 1). To minimize the interactions between the molecules, these concentrations were chosen so as to produce the absorbance less than 0.1 at the excitation wavelength. The concentrations of Au–Pd NRs varied between 7.06×10^{-6} and 1.36×10^{-4} mol/L. As seen from Table 1, we prepared thirteen different solution samples in total.

The optical absorbance and the fluorescence of our solutions were measured, using optical apparatus shown respectively in Fig. 1 and Fig. 2. A tungsten lamp ‘Mega Light100’ and a high-

Table 1. Conditions of our response surface measurements and the corresponding experimental results. Replicated runs correspond to sample numbers from #5 to #9.

Sample #	Molar concentration, mol/L			Absorbance		Integrated fluorescence, 10^5 a.u.		Refractive index n		Experimental FQY	
	Rh6G	Au-Pd NRs	Rh6G	Rh6G	Mixed solution	Rh6G	Mixed solution	Rh6G	Mixed solution	Rh6G	Mixed solution
1	3.53×10^{-7}	7.17×10^{-5}	0.022	0.119	0.50	2.29	1.3312	1.3319	0.78	0.67	
2	5.50×10^{-7}	2.60×10^{-5}	0.032	0.071	0.83	2.24	1.3322	1.3316	0.90	1.10	
3	5.50×10^{-7}	1.17×10^{-4}	0.032	0.166	0.84	2.24	1.3319	1.3321	0.90	0.47	
4	1.03×10^{-6}	7.06×10^{-6}	0.058	0.075	1.60	2.42	1.3324	1.3322	0.97	1.12	
5	1.03×10^{-6}	7.17×10^{-5}	0.058	0.155	1.58	2.75	1.3319	1.3318	0.95	0.62	
6	1.03×10^{-6}	7.17×10^{-5}	0.059	0.158	1.61	2.78	1.3316	1.3319	0.95	0.61	
7	1.03×10^{-6}	7.17×10^{-5}	0.057	0.157	1.59	2.82	1.3319	1.3317	0.97	0.63	
8	1.03×10^{-6}	7.17×10^{-5}	0.058	0.157	1.61	2.80	1.3322	1.3324	0.97	0.63	
9	1.03×10^{-6}	7.17×10^{-5}	0.067	0.159	1.81	2.79	1.3326	1.3316	0.94	0.61	
10	1.03×10^{-6}	1.36×10^{-4}	0.058	0.216	1.56	2.15	1.3315	1.3318	0.94	0.35	
11	1.50×10^{-6}	2.60×10^{-5}	0.082	0.116	2.24	3.13	1.3335	1.3326	0.96	0.95	
12	1.50×10^{-6}	1.17×10^{-4}	0.081	0.225	2.21	2.56	1.3323	1.3339	0.96	0.40	
13	1.70×10^{-6}	7.17×10^{-5}	0.096	0.194	2.60	3.20	1.3317	1.3321	0.95	0.58	

power LED (the wavelength 525 nm and the optical power 1.4 mW) were used as excitation sources for the absorbance and fluorescence measurements, respectively. The spectra were recorded with an optical spectrometer 'Avantes'. The Rh6G solution with the concentration 1.0×10^{-6} mol/L was taken as a reference. Its absorbance was equal to 0.055, the integrated relative fluorescence intensity was 1.49×10^5 and the FQY amounted to 0.95 [15]. Finally, the refractive index of the reference measured with a refractometer 'ATAGA' was equal to 1.3320.

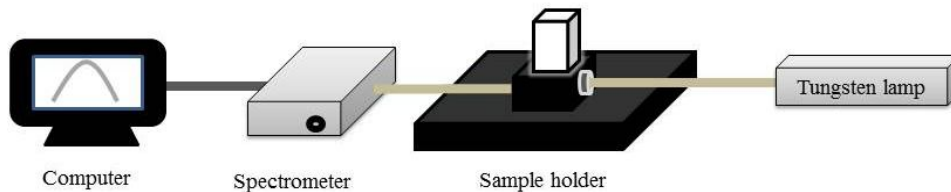


Fig. 1. Block diagram of our absorption measurement system.

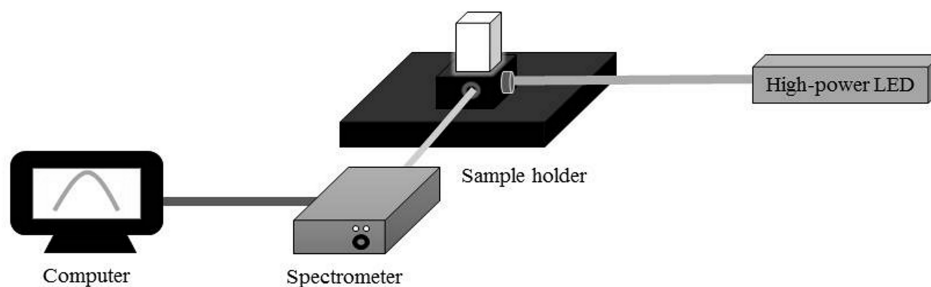


Fig. 2. Block diagram of our fluorescence measurement system.

Once the optical experiments were completed, we performed the ANOVA variance analysis to produce a prediction model. ANOVA was conducted to find out whether the model obtained from the response surface methodology was significantly reliable, or not. The modified model for estimating the response surface methodology was a quadratic polynomial given by the relation [16, 17]

$$FQY = \beta_0 + \sum_{i=1}^k \beta_i X_i + \sum_{i=1}^k \beta_{ii} X_i^2 + \sum_{i=1}^k \beta_{ij} X_i X_j . \quad (2)$$

Here FQY is the predicted FQY, X_i and X_j denote the independent variables, and β are constants. Namely, β_0 stands for the intercept, β_i the linear coefficient, β_{ii} the quadratic coefficient, and β_{ij} the interaction coefficient.

3. Results and discussion

As an example, Fig. 3a and Fig. 3b show respectively the absorption and fluorescence spectra obtained for the sample #4, both with the pure Rh6G and the Rh6G and Au–Pd NR mixture. Note that the absorption reveals a peak at about 526 nm, which is typical for all of our samples. The fluorescence peak observed at about 556 nm (see Fig. 3b) also refers to all of the samples. These peaks are therefore used to calculate the FQY according to Eq. (1).

The FQY values calculated for all of our samples are summarized in Table 1. One can see that adding of Au–Pd NRs affects efficiently both the absorbance and the fluorescence. Eventually, the first fact is evident since any scattering particles increase the light path through a cuvette, resulting in a relevant FQY change.

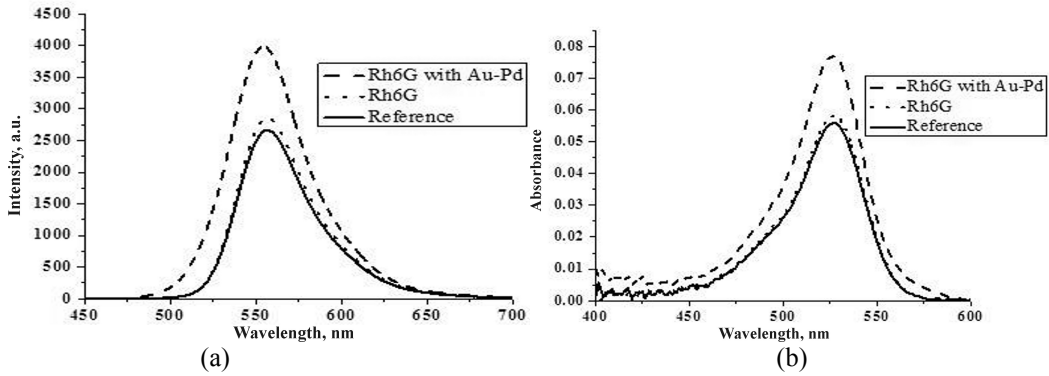


Fig. 3. Absorption spectra (a) obtained for the reference, the pure Rh6G and the mixed solution of Rh6G with Au–Pd NRs, and fluorescence spectra (b) obtained for the reference, the pure Rh6G and the same mixed solution. All of the spectra correspond to sample #4.

Now we apply the response surface approach to fit the concentration dependence. Fig. 4a shows the relationship between the empirical FQY and the FQY value predicted by the analysis of variance. The FQY dependence on the concentrations of Rh6G and Au–Pd NRs can be written as

$$\begin{aligned}
 FQY = & 1.48345 - (2.93524 \times 10^5 \times A) - (11949.31203 \times B) + (9.20837 \times 10^8 \times A \times B) \\
 & + (6.64820 \times 10^{10} \times A^2) + (3.34804 \times 10^7 \times B^2)
 \end{aligned} \quad (3)$$

where A and B represent the concentrations of Rh6G and Au–Pd NRs in mol/L, respectively. The analysis of this model has given the R^2 parameters and the p -values (see Ref. [16]), which are displayed in Table 2. When compared with the experimental data, the mathematical model given by Eq. (3) should be deemed acceptable. Indeed, the R^2 parameter is equal to 0.9923, thus confirming that the model is statistically reliable.

Table 2. ANOVA variance analysis for our quadratic response surface model: df denotes the number of degrees of freedom, F -value is the random variable from the F -distribution, and p -value the probability.

Source	Sum of squares	df	Mean square	F -value	p -value
Model	0.690	5	0.140	129.45	< 0.0001
$A = \text{Rh6G}$	0.015	1	0.015	14.05	0.0072
$B = \text{Au–Pd NRs}$	0.640	1	0.640	599.73	< 0.0001
AB	1.60×10^{-3}	1	1.60×10^{-3}	1.49	0.2616
A^2	1.56×10^{-3}	1	1.56×10^{-3}	1.46	0.2664
B^2	0.034	1	0.034	31.77	0.0008
*Residual sum of squares	7.51×10^{-3}	7	1.07×10^{-3}	–	–
Lack of fit sum	7.11×10^{-3}	3	2.37×10^{-3}	23.70	0.0052
Pure error sum	4.00×10^{-4}	4	1.00×10^{-4}	–	–
Corrected total	0.700	12	–	–	–

*Residual sum of squares is a combination of pure error sum of squares and lack of fit sum of squares

The ANOVA yields in a response surface plot shown in Fig. 4b. The FQY decreases with increasing concentration of Au–Pd NRs. In other words, addition of Au–Pd NRs into Rh6G results in reduced FQY, as compared with the pure Rh6G for which we have a typical value of 0.95 [15]. This is understood as a result of nonradiative energy transfer between the Rh6G dye and the Au–Pd NRs. In simple terms, the Au–Pd NRs act as a fluorescence quencher. One can notice the FQY values larger than unity for the samples #2 and #4. In fact, these data points remain within the

limits of experimental errors, which are typically equal to 10%. The two following factors contribute mainly to the FQY uncertainty. The first of them is fluctuations of spectral radiance of exciting light and changes in ambient temperature. The second is Rayleigh scattering at our metal nanoparticles, of which sizes are smaller than the light wavelength. The incoming light is therefore elastically scattered by the Au–Pd NRs, and the scattered light does not easily reach a photodetector. Hence, the light scattering at relatively short wavelengths can result in the absorbance tails.

As evidenced by the ANOVA (see Table 2), our model appears to be reliable for expressing the relationship between the FQY and the proportions of Rh6G and Au–Pd NRs. In particular, the p -value is less than 0.0001 and the F -value amounts to 129.45 [18].

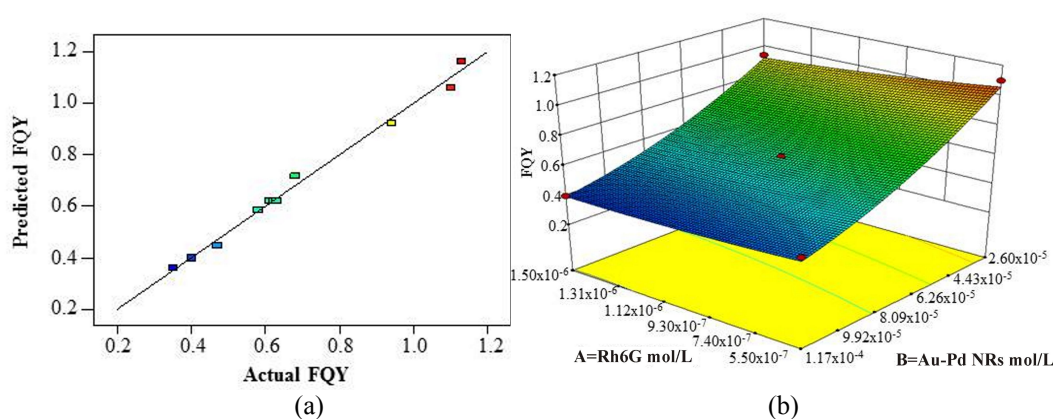


Fig. 4 (a) Correlation of actual and predicted FQY values, and (b) response surface plot obtained for the dependence of FQY on the Rh6G (A) and Au–Pd NR (B) concentrations.

To check reliability of Eq. (3), we have additionally studied the FQY from different samples that deviate from the conditions provided by the model in Table 1. The information on these samples is gathered in Table 3. We find that the discrepancies of the predicted and measured FQYs are less than 2%. This implies that the equation derived from this model is accurate and reliable enough to predict the relationship between the FQY and the concentrations of Rh6G and Au–Pd NRs in the solution.

Table 3. Comparison of empirical and theoretical FQY values obtained for our Rh6G and Au–Pd NR solutions.

Sample #	Molar concentration, mol/L		FQY for the system of Rh6G and Au–Pd NRs		Error, %
	Rh6G	Au–Pd	Model	Measured	
14	6.00×10^{-7}	3.00×10^{-5}	1.00	1.02	–2.0
15	9.00×10^{-7}	6.00×10^{-5}	0.71	0.70	1.41
16	1.20×10^{-6}	8.00×10^{-5}	0.55	0.56	–1.82

4. Conclusion

In this work we report the studies of the influence of Rh6G and Au–Pd NR concentrations on the FQY, which are performed using the response surface methodology. Our experiments have demonstrated that the FQY is sensitive to the concentrations of Rh6G and Au–Pd NRs. The dependence of FQY on the Rh6G and Au–Pd NR concentrations is derived using a general

quadratic-polynomial model. A comparison of the empirical and theoretical FQYs testifies that the errors of the model are less than 2%.

Acknowledgements

This work has been supported by the Faculty of Science, King Mongkut's Institute of Technology Ladkrabang, under the Grant Number 2560-01-05-054.

References

1. Menendez-Miranda M, Costa-Fernandez J M, Encinar J R, Parak W J and Carrillo-Carrion C, 2016. Determination of the ratio of fluorophore/nanoparticle for fluorescence-labeled nanoparticles. *Analyst*. **141**: 1266–1272.
2. Mingcong Rong, Zhixiong Cai, Lei Xie, Chunshui Lin, Xinhong Song, Feng Luo, Yiru Wang and Xi Chen, 2016. Study on the ultrahigh quantum yield of fluorescent P,O-g-C3N4 nanodots and its application in cell imaging. *Chem. - A Europ. Journ.* **22**: 9387–9395.
3. El-Bashir S M, Barakat F M and AlSalhi M S, 2013. Metal-enhanced fluorescence of mixed coumarin dyes by silver and gold nanoparticles: towards plasmonic thin-film luminescent solar concentrator. *J. Lumin.* **143**: 43–49.
4. Lee J, Lee S, Jen M and Pang Y, 2015. Metal-enhanced fluorescence: wavelength-dependent ultrafast energy transfer. *J. Phys. Chem. C*. **119**: 23285–23291.
5. Acuna G P, Bucher M, Stein I H, Steinhauer C, Kuzyk A, Holzmeister P, Schreiber R, Moroz A, Stefani F D, Liedl T, Simmel F C and Tinnefeld P, 2012. Distance dependence of single-fluorophore quenching by gold nanoparticles studied on DNA origami. *ACS Nano*. **6**: 3189–3195.
6. Suslov A, Lama P T and Dorsinville R, 2015. Fluorescence enhancement of rhodamine B by monodispersed silver nanoparticles. *Opt. Commun.* **345**: 116–119.
7. Chen Y-C, Gao C-Y, Chen K-L, Meen T-H and Huang C-J, 2013. Enhancement and quenching of fluorescence by silver nanoparticles in organic light-emitting diodes. *J. Nanomater.* **2013**: 84136.
8. Boonpipobanun N, Damrongsak P and Locharoenrat K, 2016. Comparison of fluorescence behaviors of rhodamine 6G with palladium-coated gold nanorods in formations of solutions and thin films. *Appl. Mech. Mater.* **851**: 14–18.
9. Nagaraja D, Melavanki R M, Patil N R and Kusanur R A, 2014. Solvent effect on the relative quantum yield and fluorescence quenching of 2DAM. *Spectrochem. Acta. A*. **130**: 122–128.
10. Wurtha C, Gonzalez M G, Niessner R, Panne U, Haisch C and Genger U R, 2012. Determination of the absolute fluorescence quantum yield of rhodamine6G with optical and photoacoustic methods – providing the basis for fluorescence quantum yield standards. *Talanta*. **90**: 30–37.
11. Omolola A O, Jideani A I O, Kapila P F and Jideani V I, 2015. Optimization of microwave drying conditions of two banana varieties using response surface methodology. *Food Sci. Technol.* **35**: 438–444.
12. Khumtong T, Sakulkalavek A, Sakdanuphab R, 2017. Empirical modeling and optimization of pre-heat temperature and Ar flow rate using response surface methodology for stoichiometric Sb₂Te₃ thin films prepared by RF magnetron sputtering. *J. Alloy. Compd.* **715**: 65–72.
13. Babaki M, Yousefi M, Habibi Z and Mohammadi M, 2017. Process optimization for biodiesel production from waste cooking oil using multi-enzyme systems through response surface methodology. *Renew. Energ.* **105**: 465–472.

14. Chaisongkroh N, Chungsiriporn J and Bunyakan C, 2012. Modeling and optimization of ammonia treatment by acidic biochar using response surface methodology. Songklanakarin J. Sci. Technol. **34**: 423–432.
15. Zang X-F, Zhang Y and Liu L, 2014. Fluorescence life times and quantum yields of ten rhodamine derivatives: Structural effect on emission mechanism in different solvents. J. Lumin. **145**: 448–453.
16. Noshadi I, Amin N A S and Richard S P, 2012. Continuous production of biodiesel from waste cooking oil in a reactive distillation column catalyzed by solid heteropolyacid: Optimization using response surface methodology (RSM). Fuel. **94**: 156–164.
17. Mandala D K, Bhunia H, Bajpai P K, Kushwaha J P, Chaudhari C V, Dubey K A and Varshney L, 2017. Optimization of acrylic acid grafting onto polypropylene using response surface methodology and its biodegradability. Radiat. Phys. Chem. **132**: 71–81.
18. Danmaliki G I, Saleh T A and Shamsuddeen A A, 2017. Response surface methodology optimization of adsorptive desulfurization on nickel/activated carbon. Chem. Eng. J. **313**: 993–1003.

Ekkachai Rammarat, Kitsakorn Locharoenrat, Witoon Yindeesuk and Pattareeya Damrongsak. 2017. Studies of concentration dependence of the fluorescent quantum yield from rhodamine 6G and Au–Pd core–shell nanorods, using a response surface methodology. Ukr.J.Phys.Opt. **18**: 179–186.

***Анотація.** У цій праці застосовано підхід поверхні відгуку до вивчення квантового виходу флуоресценції (КВЛ) родаміну 6G (Р6G), змішаного з нанопаличками Au–Pd типу серцевина-оболонка (Au–Pd НП). КВЛ було виміряно для концентрацій Р6G у діапазоні від $3,53 \times 10^{-7}$ до $1,70 \times 10^{-6}$ моль/л і концентрацій Au–Pd НП від $7,06 \times 10^{-6}$ до $1,36 \times 10^{-4}$ моль/л. Експериментальні результати засвідчили, що КВЛ істотно залежить від пропорцій Р6G і Au–Pd НП. Конкретний взаємозв'язок між КВЛ і концентраціями також підтверджено графіком поверхні відгуку. Виявлено, що розбіжність між експериментом та розрахунком складає менше 2%.*